Title	Switchable release nano-reservoirs for co-delivery of drugs via a facile micelle-hydrogel composite
Author(s)	Patel, Monika; Kaneko, Tatsuo; Matsumura, Kazuaki
Citation	Journal of Materials Chemistry B, 5(19): 3488-3497
Issue Date	2017-04-12
Type	Journal Article
Text version	author
URL	http://hdl.handle.net/10119/15285
Rights	Copyright (C) 2017 Royal Society of Chemistry. Monika Patel, Tatsuo Kaneko and Kazuaki Matsumura, Journal of Materials Chemistry B, 5(19), 2017, 3488-3497. http://dx.doi.org/10.1039/C7TB00701A - Reproduced by permission of The Royal Society of Chemistry
Description	

Journal Name

ARTICLE

Switchable Release Nano-Reservoirs for Co-Delivery of Drugs via a Facile Micelle-Hydrogel Composite

Monika Patel,[a] Tatsuo Kaneko[b] and Kazuaki Matsumura[a]

Precise and controlled drug delivery systems are required to facilitate effective therapeutics. To address this need, we devised a micelle-hydrogel composite based on amphiphilic polypeptides as a general carrier model for the switchable and controlled release of dual drugs. Two different di-block polypeptides, poly (L-lysine-b-L- phenylalanine) and poly (L-glutamic acid-b-L-phenylalanine) (PGA-PPA), were synthesized to form distinct self-assembling micellar systems that were loaded with curcumin and amphotericin B, respectively, as model drugs. The drug-loaded micellar mixture was crosslinked utilizing the pendant amino groups of the L-lysine side chains via genipin to yield a micelle-hydrogel composite with PGA-PPA micelles trapped in the interlinked hydrogel system. This composite allowed for controlled multiphasic drug release and could be effectively tuned to moderate the pace and amount of drug release and be easily regulated to switch the drug release kinetics over a range of simple factors such as change in pH, cross-linking density, and composition.

Introduction

Complications in the treatment of advanced disease have highlighted the requirement for drug co-administration in a dose-controlled manner. Conventional forms of drug administration often necessitate higher dose or recurrent administration to yield desired therapeutic effects, potentially resulting in lower efficacy and patient compliance as well as adverse effects and induced toxicity.[1] Conversely, combination therapies utilizing multiple drugs concurrently may enhance the progression of treatment as well as tissue regeneration in cases of injury or trauma.[2] To improve these effects, different drug formulations should be administered at their optimal dose and treatment exposure periods. However, simple drug delivery systems only partly fulfill these needs independently; thus, controlled dual drug release systems are required. Although a few studies have addressed the fabrication of dual drug delivery systems (DDS),[3] controllability over the release of the second drug has remained an issue,[4] limiting the purpose of dual delivery and potentially yielding adverse effects from drug overexposure.

The majority of reported dual DDS contain hydrogel as a primary component of drug encapsulation. Since the first synthetic hydrogels were formulated,[5] the use of hydrogel technology has been broadened to many fields including food additives,[6] regenerative medicine,[7] tissue engineering,[8] diagnostics,[9] biomedical implants,[10] as well as pharmaceuticals[11] and drug delivery.[12] Hydrogels comprise three-dimensional network structures possessing unique properties such as porosity, strength, and swelling in aqueous environments that can be tuned over a wide range of parameters, making them ideal for use in DDS.[13] However, for biological and drug delivery purposes, the range of natural as well as synthetic hydrophilic polymers is restricted based on their biocompatibility and biodegradability. Notably, hydrogels based on poly amino acids (homo-, di-, or multi-block polymers)[14] have recently emerged as promising physical candidates especially suitable for controlled drug delivery owing to their ready formation, assembly, and stimuli responsiveness.[15] However, these hydrogels also exhibit limitations like the slow and inefficient uptake of drugs by sorption and limited loading potential especially for hydrophobic drugs.[16] Furthermore, the crosslinking reaction may conjoin the drug to the hydrogel or compromise its chemical integrity, restricting drug delivery, whereas the hydrogel itself may exhibit non-biodegradability and composition problems

As an alternative, polymeric micelle-based DDS[17] offer the ease of self-assembly, exhibit distinct stability in soluble states, and contain well-defined hydrophobic and hydrophilic domains that markedly improve hydrophobic drug solubility, allowing high drug loading capability. Conversely, limitations include overall micelle stability, dose control, long-term release, and site specific drug delivery. However, recent advances in establishing complex DDS suggest the potential for developing a delivery formulation providing simultaneous gelation and a better degree of drug loading in an aqueous environment.

Accordingly, we aimed to design a system capable of sustaining hydrogel integrity as well as providing better controllability over drug release through drug encapsulation in micellar nano-reservoirs. The amphiphilic di-block polypeptide-based micelle-hydrogel[18] composite described here integrates

[a.] Materials Chemistry Area, School of Materials Science,
Japan Advanced Institute of Science and Technology, 1-1 Asahidai, Nomi, Ishikawa 923-1292, Japan. E-mail: mkazuaki@jaist.ac.jp
[b] Energy and Environment Area, School of Materials Science,
Japan Advanced Institute of Science and Technology

these two strategies (micelles and hydrogels) in a single entity for controlled and switchable drug co-delivery.

Experimental

Materials

ε-Benzyloxycarbonyl-L-lysine (H-Lys (Z)-OH), γ-benzyl-L-glutamic acid (H-Glu (OBzl)-OH), phenylalanine (H-phe-OH), trifluoroacetic acid, and 30% hydrogen bromide (HBr) in acetic acid were purchased from Watanabe Chemical IND., Ltd. (Hiroshima, Japan). N, N-dimethylformamide (DMF) anhydrous, hexane (anhydrous), and tetrahydrofuran (THF) were acquired from Kanto Chemical Co., Inc. (Tokyo, Japan). Diethyl ether and dimethyl sulfoxide (DMSO) were bought from Nacalai Tesuque (Kyoto, Japan). Triphosgene and curcumin (Cur) were purchased from Tokyo Chemical Industry Co., Ltd. (Tokyo, Japan). Amphotericin B (AmpB) and genipin were purchased from Wako Pure Chemical Industries, Ltd. (Osaka, Japan) and Amatek Chemical Co., Ltd. (Hong Kong,) respectively. Phosphotungstic acid was bought from Sigma Aldrich (Tokyo, Japan). All chemicals were used as received.

Methods

Synthesis of N-carboxyanhydrides of Amino Acids. Synthesis of N-carboxyanhydrides (NCA) of L-lysine (Lys (Z)-NCA), L-glutamic acid (Glu (OBzl)-NCA), and L-phenylalanine (Phe-NCA) was performed using the protocol reported by Farthing and Reynolds[19] using triphosgene. Briefly, for the preparation of Lys (Z)-NCA, Lys (Z)-OH (3 g, 10.71 mmol) was suspended in a two-neck flask in tetrahydrofuran (THF) (30 mL). Triphosgene (3.17 g, 10 mmol) in THF (20 mL) was added to the suspension with stirring at 50 °C under reflux for 3 h until the solution turned clear. After 3 h, the excess phosgene was removed from the solution under reduced pressure. The crude product thus obtained was re-suspended in THF and was poured in n-hexane to yield a white precipitate that was recrystallized twice in a mixture of THF/n-hexane. Yield: 2.3 g; 7.5 mmol; 75%. ^{1}H-NMR (400 MHz, dimethylsulfoxide (DMSO)-d$_6$, 25 °C): 1.29–1.44 (m, 4H, J=7.2 Hz), 1.56–1.82 (m, 2H, J=6.7 Hz), 3.01 (q, 2H, J=5.3 Hz), 4.43 (t, 1H, J=6.2), 5.03 (s, 1H), 7.37 (m, 5H, J= 7.1 Hz), 9.011 (s, 1H). ^{13}C-NMR (400 MHz, DMSO-d$_6$): 21.66 (s), 28.82 (s), 30.69 (s), 40.3 (s; masked by DMSO multiplet), 57.07 (s), 65.19 (s), 127.78 (s), 127.83 (s), 128.40 (s), 137.31 (s), 152.04 (s), 156.16 (s), 171.72 (s).

Glu(OBzl)-NCA and Phe-NCA were also prepared following a similar protocol.

Glu(OBzl)-NCA Yield: 2.12 g; 8.01 mmol; 64%. ^{1}H-NMR (400 MHz, DMSO-d$_6$, 25 °C, TMS): 1.07–1.25 (m, 2H, J= 5.4 Hz), 1.68 (t, 2H, J= 6.1 Hz), 3.63 (t, 1H, J= 7.8 Hz), 4.24 (s, 2H), 6.52 (m, 5H, J= 5.9 Hz), 8.25 (m, 1H, J=7.4 Hz). ^{13}C-NMR (400 MHz, DMSO-d$_6$): 26.45 (s), 29.11 (s), 56.24 (s), 65.75 (s), 125.03 (s), 128.10 (s), 128.49 (s), 136.05 (s), 151.91 (s), 171.38 (s), 171.75 (s).

Phe-NCA Yield: 2.43 g; 12 mmol; 82%. ^{1}H-NMR (400 MHz, DMSO-d$_6$, 25 °C): 3.04–3.23 (m, 2H, J= 6.9 Hz), 4.82 (t, 1H, J= 8.3 Hz), 7.37 (m, 5H, J=5.1 Hz), 9.62 (s, 1H). ^{13}C-NMR (400 MHz, DMSO-d$_6$): 35.64 (s), 66.08 (s), 128.29 (s), 128.53 (s), 128.98 (s), 136.91 (s), 154.01 (s), 170.72 (s).

Synthesis of PLL-PPA and PGA-PPA Di-block Copolymers. The block copolymers PZLL-*b*-PPA and P(OBzl)GA-*b*-PPA were synthesized in a two-step process: firstly, the hydrophilic block (of either glutamic acid or lysine) was synthesized by ring-opening polymerization of the respective NCA. For this, 7 mmol Lys (Z)-NCA (2 g)/Glu (OBzl)-NCA (1.8 g) was dissolved in 5 mL dimethylformamide with n-hexylamine (9.5 μL, 0.07 mmol) used as the initiator and stirred for 48 h at room temperature. Upon complete utilization of the first block monomer, Phe-NCA (0.67 g, 0.35 mmol) was added as the second hydrophilic block and stirred for another 36 h, and then precipitated with an excess of diethyl ether under vigorous stirring. Then, the viscous polymer was again dissolved in dimethylformamide and re-precipitated with diethyl ether to give a white solid of PZLL-PPA or P(OBzl)GA-PPA. The polymers were dried under vacuum at room temperature. De-protection was performed by dissolving the polymers in trifluoroacetic acid and 33% HBr/CH$_3$COOH followed by stirring for 10 h at room temperature. The de-protected polymers were precipitated with an excess of diethyl ether to obtain white solids that were dried in vacuum at room temperature for 48 h to yield PLL-PPA and PGA-PPA.

Characterization. ^{1}H and ^{13}C NMR spectra were obtained at 25 °C on a Bruker AVANCE III 400 spectrometer (Bruker BioSpin Inc., Fällanden, Switzerland) in d$_6$-DMSO. Gel permeation chromatography (GPC) measurements were performed before de-protection of the polypeptides using a Shodex GPC101 (Yokohama, Japan) with a connection column system of 803 and 807 and equipped with Jasco 830 RI and Jasco UV-2075 plus detectors using pullulan as a molecular weight standard. Transmission Electron Microscopy (TEM) was performed using a Hitachi H-7100 TEM (Tokyo, Japan). Samples were prepared by adding the micellar solution onto a copper mesh and allowing it to dry. The dried sample was stained with phosphotungstic acid and observed.

Formation of Micelles. For the preparation of micelles (empty), a 2% (w/v) solution of amphiphilic polypeptide was prepared separately in DMSO and stirred for 2 h to ensure complete dissolution. This solution was then dropped into distilled water under continuous stirring. The resulting solution was transferred into a dialysis bag (MWCO 3500) and dialyzed against distilled water with a change in solvent 2–3 times a day for 2 days.

Critical Micellar Concentration (CMC) Determination. Pyrene was used as a hydrophobic probe for the determination of CMC values of the PLL-*b*-PPA and PGA-*b*-PPA micelles. Pyrene solution in acetone (100 μL, 6×10^{-6} mol L^{-1}) was added into two sets of aliquots and the acetone was allowed to evaporate.

Then, 1.0-mL micellar (PLL-PPA or PGA-PPA) solutions at various concentrations were added to the aliquots and incubated overnight with continuous shaking. Pyrene was excited at 334 nm using a Jasco FP-8600 spectrofluorometer (Oklahoma City, OK, USA). A red shift in the excitation peak was observed upon varying the concentration of the polymer. The ratio of fluorescence intensity as a function of log of concentration of polymer was plotted to determine the CMC value.

Stability. Micelle size was measured on a Malvern Zetasizer Nano ZS (Malvern, UK). For stability testing, the micelle solutions were prepared and micelle size was measured in a polystyrene cuvette over 7 days. For drug loaded micelles, the loaded micelles were suspended in phosphate buffered saline (PBS) buffer and size was recorded over 2 weeks. All samples had a concentration of approximately 1 mg mL^{-1} and were filtered through an 0.8-μm Millex GP filter (Merck Millipore Ltd., Billerica, MA, USA) prior to measurement.

Loading of AmpB and Cur in Micelles. For drug loading, 20 mg AmpB/Cur were dissolved in 2 mL DMSO. Then, 100 mg polymer solution was added to the prepared drug solution and stirred for 2 h. The polymer and drug solution was next added to 10 mL distilled water dropwise with continuous stirring. The obtained solution was lyophilized using the freeze dry method for storage and further use.

Drug loading Efficiency. To determine loading efficiency, 10 mg drug-loaded micelles were weighed into a mini centrifuge tube and reconstituted in 500 μL DMSO for complete dissolution of micelles into free polymers. After filtration, the concentration was recorded using a UV-Vis spectrophotometer. AmpB concentration was measured by spectroscopy at 368 nm and Cur was measured at 426 nm against a standard calibration curve.[20] The following formula was used for calculation:

$$\% \text{ Loading efficiency} = \frac{\text{amount of drug in micelles}}{\text{amount of total drug loaded}} \times 100 \quad (1)$$

Preparation of Hydrogels. The hydrogels were prepared by cross-linking between genipin and the amino group in PLL-*b*-PPA polymers. The freeze-dried drug-loaded micelles were dissolved in deionized water (2% w/v of each) and the resultant solutions were stirred for at least 2 h to ensure that the polypeptides were dissolved in completely. Genipin (0.5–2.5 %w/v) was mixed with the polypeptide solution and was allowed to stand for 20 h to form dark blue hydrogels. The gelation and time of gelation of the cross-linked polypeptide hydrogels were investigated using the vial tilting method.

Drug Release. A standard shape (circular disc with height of 5 mm) of micelle-hydrogel was cut using a punch of 10 mm diameter and was immersed in 50 mL PBS. The PBS was subsequently changed every 4 h and the collected PBS was used to measure the amount of drug at fixed time points using spectroscopy. The standard sample was prepared by dissolving both Amp B and Cur and recording standard curves at different λ_{max} for both Cur and Amp B to account for the interference

arising from the action of one drug on another during the recording of absorbance in the dual drug release studies.

Swelling Study. The swelling ratios of genipin cross linked micelle-hydrogels composites were measured at 37 °C. Equal size (circular disc of diameter 10 mm and height 5 mm) hydrogel samples were punched from fresh made composites and were weighed and immersed in PBS at pH 7.4 for 24 h. Then, the samples were gently removed from the buffer and gently wiped with filter paper to remove the excess buffer on the surface. These composites were then weighed. The swelling percentage was calculated as follows:

$$\text{Swelling Percentage} = \frac{Wt - Wo}{Wo} \times 100 \quad (2)$$

Here, Wo denotes the weight of the composite before swelling and Wt is weight of composite after 24 h swelling in the buffer.

Circular Dichorism. The secondary structure changes of the synthesized polypeptides were studies by far-UV circular dichroism (CD) spectra before and after pH treatment. The protein concentration and path length of the cell used were polypeptides were solution of 20 μM was prepared and the spectrum was recorded in a cuvette of path length 0.5 cm, using a JASCO-820 spectropolarimeter. Each spectrum was baseline-corrected and was collected as an average of three scans at a scan rate of 200 nm min^{-1} and a response time of 2 s.

Results and discussion

We successfully employed the highly condensed ampholytic micelles and demonstrated controlled dual drug release from their core. As shown in **Figure 1**, the proposed micelle-hydrogel composite constitutes two distinct drug-loaded nano-reservoirs (differently charged in differing crosslinking environments), providing mutually exclusive drug release profiles beneficial for synergistic wound healing. The drug-loaded composites were characterized for drug release profile switching ability in vitro under various pH, composition, and cross linking conditions to provide sufficient groundwork for clinical trials.

A facile fabrication strategy was followed to develop micelle-hydrogel composite development. Briefly, two different amphiphilic di-block polypeptides were synthesized (**Figure 1**a) in *N,N*-dimethylformamide by ring opening polymerization[21] using Nε-benzyloxycarbonyl-L-lysine-Nα-carboxy anhydride (Lys (Z)-NCA) and L-phenylalanine NCA (Phe-NCA) to yield the cationic amphiphile poly (L-lysine-*b*-L-phenyl alanine) (PLL-PPA), and with γ-benzyl-L-glutamate NCA (Glu (OBzl)-NCA) and Phe-NCA yielding poly (L-glutamic acid-*b*-L-phenylalanine) (PGA-PPA) as the anionic amphiphile (after subsequent de-protection) at ambient temperature as shown in Scheme 1. The synthesized NCA monomers were characterized using ^{1}H-NMR and ^{13}C NMR (**Figure S1** and **S2**) and di-block polypeptides were characterized by ^{1}H-NMR and GPC (**Table 1** and **Figure S3**). The polypeptide molecular weight was

controlled by the initiator to monomer molar ratio and examined using a time course study showing well-controlled polymer molecular weights with narrow polydispersity index (**Figure S4**). Among all the synthesized polypeptides, the polypeptides with hydrophilic to hydrophobic block ratio of 100:5 were used for preparing micelle-hydrogel composites and investigating in-vitro dual drug release. This ratio of hydrophilic to hydrophobic group was optimized studying the solubility of the synthesized polymers in water, as the polymers with higher than 5 mole percent of PPA tend to be less soluble in water and showed considerably higher CMC. These di-block polypeptides readily self-assembled into micelles in aqueous solution (**Figure 1**b); micelle morphology was studied using TEM and dynamic light scattering (DLS), revealing a spherical shape for both (**Figure 2**). Average hydrodynamic diameters were 170 and 195 nm for PGA-PPA and PLL-PPA, respectively, at physiological pH (**Figure S5**) vs. 10–15 nm in TEM, wherein the charged shell (PLL/PGA) block was dehydrated and thus packed in tightly coiled helices, which on interaction with water swelled considerably (10–15 times their original diameter). [22]

To confirm this swelling behavior, micelle size was studied at various pH, with substantial size decrease upon transition from charged to uncharged states (e.g., PLL-PPA hydrodynamic diameter of 102 nm at pH 9.0 and PGA-PPA diameter of 76 nm at pH 4.0 (**Figure S5 e and f**). A critical micelle concentration (CMC) value of 0.15 and 0.22 mg mL^{-1} was seen for PGA$_{100}$-PPA$_5$ and PLL$_{100}$-PPA$_5$ (subscripts indicating the block ratio at feed) respectively (**Figure 3**).

However, although block copolymers with smaller block sizes, especially the hydrophobic block (as herein) may show a higher CMC in water, the PLL-PPA and PGA-PPA di-blocks showed a low formed micelle CMC value, indicating high polypeptide micellization efficiency through π-π stacking[23] of the benzyl groups of the phenyl alanine block in the core, and also leading to high stability. In colloidal systems, the ζ-potential predicts stability in terms of suspension aggregation, with a stable system exhibiting a ζ -potential magnitude > ±30 mV.[24] Here, DLS also showed micelle stability as a function of size, with fair stability in aqueous solution over 14 days with minimal degradation or aggregation (**Figure 4**). This may be attributed to the highly charged shells, arising from ionizable side chain groups in the hydrophilic part of the polypeptides yielding a ζ-potential of 68 and –63 mV at physiological pH for PLL$_{100}$-PPA$_5$ and PGA$_{100}$-PPA$_5$, respectively, repelling any between-micelle ionic interactions.[25]

To assess the potential of the DDS for delivery of wound healing agents, the prepared micelle cores were used as nano-reservoirs for the model drugs curcumin (Cur) and amphotericin B (AmpB) to generate the drug-loaded micelle-hydrogel composites, with high loading efficiency (76.5% and 87.4%) in PLL-PPA and PGA-PPA, respectively. Cur has been shown to have efficacy toward wound healing[26] and AmpB was used as a model fungicidal drug, critical for preventing topical wound sepsis.[27] These core-loaded nano-reservoirs were then

crosslinked using the free -NH$_2$ (**Figure 1**c) groups in the PLL-PPA micelle shell via the water soluble biocompatible cross linker genipin[28] to form a hydrogel network of characteristic dark blue color with free PGA-PPA micelles trapped inside the network. The sol to gel transition was confirmed by the tube inversion method and stable self-standing gels were observed (**Figure 1**d).

Because of the ionizable properties of the micelle-hydrogel composites, we next investigated their pH responsiveness. A 4% w/v (2% each of PLL-PPA and PGA-PPA) micellar mixture was gelled using 1.0% genipin; this gelation condition was used throughout study unless stated otherwise, and was then subjected to drug release assessment in different pH environments (pH 3, 7, and 11) (**Figure 5**a and b). The drug release profile clearly indicated that the drug loaded composite was susceptible to change in pH. The cationic PLL-PPA micelles showed a rushed release of Cur at pH 11, with a slower release at lower pH. In contrast, PGA-PPA micelles showed an opposite trend with burst release at pH 3 and an extended release profile at higher pH. As the PLL and PGA blocks surpassed their respective pKa (8.2 and 4.3) and moved to a relatively uncharged state, both lysine and glutamic acids, which are known for their helix forming ability in an uncharged state,[29] attained a helix conformation. Change in pH from 3 to 11 caused rapid deprotonation of L-lysine side chains in micelles; a similar transition was seen for PGA upon pH change from 11 to 3, whereupon the carboxylic groups of glutamic acid side chains gained a proton to become neutral. Advancement from charged to uncharged states changed the micelle hydrophilic chain conformations. The random coil states tended to form a highly ordered helix conformation causing shrinking of the hydrophilic segment with marked decrease in the water solubility.[30] This transition can be clearly seen in the change in the CD spectra of the polypeptides at different pH (**Figure S6**). This, thus generates a strain on the micellar core, resulting in rapid drug leakage from the micelles. As both micelles showed this transition going toward the opposite end of the pH scale, a reverse trend in micellar behavior was recorded that could be switched by changing the pH (**Figure 5**c and d). To further confirm our assumptions regarding the switchability in terms of drug release profile, we subjected the composites to a sudden change in pH and studied the cumulative release rate. As seen in **Figure 5**e and f, a biphasic release curve was observed with a sudden jump in release rate when subjected to drastic pH changes, which supported our claim. Although this outcome is not closely related to the biological environment as such drastic pH difference is rarely observed *in vivo*, the switchable profile of the prepared composite through environmental changes including pH is notable. Therefore, the feature of environmentally responsive switchability allows drug delivery systems to be dramatically controlled with respect to their swelling behavior, drug permeability, and release profile in response to variations in the pH or ionic strength of the surrounding fluid, which may be useful for modulated drug delivery.

To better understand the switching ability of the formed composites for drug release, we investigated their drug release profiles over various crosslinking densities by using cross linker concentrations at 0.5, 1, 2.5, and 5%. This yielded opposite trends in drug release pattern at pH 7.4 for both micelle groups. Cur loaded in PLL-PPA micelles showed marked drug release rate decrease from 70 to 38% with increased cross linker concentration from 0.5 to 5% (**Figure 6**a) whereas Amp B loaded in PGA-PPA micelles showed a positive trend from 45 to 91% with increased genipin concentration, showing burst release in higher gel concentrations (2.5 and 5%) (**Figure 6**b). With increased genipin concentration, more $-NH_2$ PLL side groups are involved in inter- and intra-micelle crosslinking. And as the crosslinking density increases, the micelle shells are more stabilized to firmly hold the core. And this leads to a more stable hydrophobic core of the PLL-PGA micelles and the leaching of the drug from the core is slowed down sustainably, leading to slower drug release (figure 6 c). Oppositely as the cross linker concentration increases the PGA-PPA micelles which are trapped among the PLL-PPA crosslinked systems become extensively constrained due to lack of proper space, as the interlinking among PLL-PPA micelles increases and PGA-PPA experience a higher distorting stress as they are held in a tightly packed situation, stressing the unbound AmpB-loaded PGA-PPA micelles.[31] In turn, PGA-PPA micelles succumb to the stress[32] and core structure disruption leads to a burst release of Amp B from the micelles (Figure 6 d). Thus, two differing pharmacokinetic drug profiles occurred by changing the cross linker concentration, which may be conducive to tailoring micelle-hydrogel composites for optimum drug release over a sustained period without causing unnecessary drug leakage and thus instigating toxicity.

Finally, we examined the role of surface charges resulting from the interplay of charges in the block polypeptide shells on the composite drug release profiles. The PLL-PPA and PGA-PPA micelle composition (%w/w) was systematically varied to achieve mixed micellar solutions (1:0, 1:0.5, 1:1, 1:2, and 0:1) with charges from 68 to −63 mV (**Figure S7**). The first four systems were also crosslinked to form composites (as no $-NH_2$ groups were available for crosslinking in the 0:1 ratio) and their drug release profiles assessed at pH 7.4 (**Figure 7**). PLL-PPA micelle crosslinking provided considerable stability toward swelling upon higher positive surface charge, yielding faster drug release in 68 and 23 mV composites with no burst release; at negative surface charge, the crosslinked micelle remained unaffected by the swelling, exhibiting sustained drug release. Conversely, micelle hydrogel composites with high surface charge (both positive and negative) showed rapid AmpB release whereas those with low net charge showed sustained release. This could be due to differential composite swelling rates based on surface charge (**Figure S8**).

This kinetic trend of faster PGA-PPA drug release with higher surface charge may act as an efficient tool for dual drug delivery at wound sites to accelerate healing; as initial sepsis may delay the wound healing process.[33] A burst release of antibiotic and/or antifungal drugs in the first phase may be beneficial for avoiding sepsis in the exposed wound, whereas sustained release may aid wound closure.

Conclusion

These results indicate that our micelle-hydrogel composite, with excellent tunable properties and controllable multidrug release, may serve as a potential dual drug release system. This polypeptide-based delivery system displays distinctive advantages for clinical application, such as 1) combinational drug delivery: the dual DDS can solve the problem of substandard therapeutic effects of single DDS; 2) independent drug release: each drug can be released from the micelle-hydrogel composite system independently without affecting the release of the other; 3) tunability: our composite contains two oppositely charged polypeptide micelles that differentially interact with various environments and present distinctive, well-controlled pharmacokinetic drug release profiles; and 4) ease of handling: the micelle hydrogel composite is simple to prepare and the drug release behaviors can be easily tailored by varying composite preparation parameters. We expect that the amphiphilic polypeptide based micelle-hydrogel composite system may provide a promising solution as a dual-drug carrier with controlled release behavior of each drug for combined therapy applications.

Acknowledgements

## Disclosures

The authors have no conflicts of interest to declare.

Notes and references

1   a) T. R. Hoare, D. S. Kohane, *Polymer* **2008**, *49*, 1993-2007; b) R. Langer, *Nature* **1998**, *392*, 5-10; c) W. B. Liechty, D. R. Kryscio, B. V. Slaughter, N. A. Peppas, *Annu. Rev. Chem. Biomol. Eng.* **2010**, *1*, 149-173.

2   a) J. S. Lee, J. W. Bae, Y. K. Joung, S. J. Lee, D. K. Han, K. D. Park, *Int. J. Pharm.* **2008**, *346*, 57-63; b) L. Y. Qiu, Y. H. Bae, *Biomaterials* **2007**, *28*, 4132-4142; c) J. M. Davidson, K. N. Broadley, D. Quaglino, Jr., *Wound Repair Regen.* **1997**, *5*, 77-88.

3   a) X. Cheng, Y. Jin, T. Sun, R. Qi, H. Li, W. Fan, *Colloids Surf., B* **2016**, *141*, 44-52; b) J. A. Chikar, J. L. Hendricks, S. M. Richardson-Burns, Y. Raphael, B. E. Pfingst, D. C. Martin, *Biomaterials* **2012**, *33*, 1982-1990; c) W. Wang, E. Wat, P. C. Hui, B. Chan, F. S. Ng, C. W. Kan, X. Wang, H. Hu, E. C. Wong, C. B. Lau, P. C. Leung, *Sci. Rep.* **2016**, *6*, 24112.

4   a) B. J. Lee, S. G. Ryu, J. H. Cui, *Int. J. Pharm.* **1999**, *188*, 71-80; b) L. Wei, C. Cai, J. Lin, T. Chen, *Biomaterials* **2009**, *30*, 2606-2613; c) Z. Wu, X. Zou, L. Yang, S. Lin, J. Fan, B. Yang, X. Sun, Q. Wan, Y. Chen, S. Fu, *Colloids Surf., B* **2014**, *122*, 90-98.

5   O. Wichterle, D. Lim, *Nature* **1960**, *185*, 117-118.
6   a) N. Roy, N. Saha, T. Kitano, P. Saha, *Carbohydr. Polym.* **2012**, *89*, 346-353; b) A. Gregorova, N. Saha, T. Kitano, P. Saha, *Carbohydr. Polym.* **2015**, *117*, 559-568.
7   a) E. G. Popa, M. E. Gomes, R. L. Reis, *Biomacromolecules* **2011**, *12*, 3952-3961; b) Z. Wang, Y. Zhang, J. Zhang, L. Huang, J. Liu, Y. Li, G. Zhang, S. C. Kundu, L. Wang, *Sci. Rep.* **2014**, *4*, 7064.
8   a) S. Berski, J. van Bergeijk, D. Schwarzer, Y. Stark, C. Kasper, T. Scheper, C. Grothe, R. Gerardy-Schahn, A. Kirschning, G. Drager, *Biomacromolecules* **2008**, *9*, 2353-2359; b) F. Z. Cui, W. M. Tian, S. P. Hou, Q. Y. Xu, I. S. Lee, *J. Mater. Sci. Mater. Med.* **2006**, *17*, 1393-1401; c) K. M. Galler, J. D. Hartgerink, A. C. Cavender, G. Schmalz, R. N. D'Souza, *Tissue Eng. Part A* **2012**, *18*, 176-184.
9   a) N. Gajovic, G. Beinyamin, A. Warsinke, F. W. Scheller, A. Heller, *Anal. Chem.* **2000**, *72*, 2963-2968; b) F. Kivlehan, M. Paolucci, D. Brennan, I. Ragoussis, P. Galvin, *Anal. Biochem.* **2012**, *421*, 1-8.
10   a) Y. Akagawa, T. Kubo, K. Koretake, K. Hayashi, K. Doi, A. Matsuura, K. Morita, R. Takeshita, Q. Yuan, Y. Tabata, *J. Prosthodont. Res.* **2009**, *53*, 41-47; b) A. Ma, B. Zhao, A. J. Bentley, A. Brahma, S. MacNeil, F. L. Martin, S. Rimmer, N. J. Fullwood, *J. Mater. Sci. Mater. Med.* **2011**, *22*, 663-670;
11   a) B. Gao, T. Konno, K. Ishihara, *J. Biomater. Sci. Polym. Ed.* **2015**, *26*, 1372-1385; b) C. C. Karlgard, N. S. Wong, L. W. Jones, C. Moresoli, *Int. J. Pharm.* **2003**, *257*, 141-151.
12   a) C. Gong, S. Shi, L. Wu, M. Gou, Q. Yin, Q. Guo, P. Dong, F. Zhang, F. Luo, X. Zhao, Y. Wei, Z. Qian, *Acta. Biomater.* **2009**, *5*, 3358-3370; b) B. Xue, V. Kozlovskaya, F. Liu, J. Chen, J. F. Williams, J. Campos-Gomez, M. Saeed, E. Kharlampieva, *ACS Appl. Mater. Interfaces* **2015**, 7, 13633-13644.
13   a) V. S. Ghorpade, A. V. Yadav, R. J. Dias, *Int. J. Biol. Macromolec.* **2016**, *93*, 75-86; b) G. P. Mishra, R. Kinser, I. H. Wierzbicki, R. G. Alany, A. W. Alani, *Eur. J. Pharm. Biopharm. e.V* **2014**, *88*, 397-405.
14   a) M. B. Charati, I. Lee, K. C. Hribar, J. A. Burdick, *Small* **2010**, *6*, 1608-1611; b) Y. N. Zhang, R. K. Avery, Q. Vallmajo-Martin, A. Assmann, A. Vegh, A. Memic, B. D. Olsen, N. Annabi, A. Khademhosseini, *Adv. Funct. Mater.* **2015**, *25*, 4814-4826;
15   a) C. M. Dong, Y. Chen, *J. Control. Release.* **2011**, *152 Suppl 1*, e13-14; b) C. Li, A. Faulkner-Jones, A. R. Dun, J. Jin, P. Chen, Y. Xing, Z. Yang, Z. Li, W. Shu, D. Liu, R. R. Duncan, *Angew. Chem.* **2015**, *54*, 3957-3961;
16   a) P. Markland, Y. Zhang, G. L. Amidon, V. C. Yang, *J. Biomed. Mater. Res.* **1999**, *47*, 595-602; b) K. Men, W. Liu, L. Li, X. Duan, P. Wang, M. Gou, X. Wei, X. Gao, B. Wang, Y. Du, M. Huang, L. Chen, Z. Qian, Y. Wei, *Nanoscale* **2012**, *4*, 6425-6433.
17   a) K. Peng, I. Tomatsu, A. Kros, *J. Control. Release.* **2011**, *152 Suppl 1*, e72-74; b) W. Li, L. Huang, X. Ying, Y. Jian, Y. Hong, F. Hu, Y. Du, *Angew. Chem.* **2015**, *54*, 3126-3131; b) F. Ye, H. Guo, H. Zhang, X. He, *Acta Biomater.* **2010**, *6*, 2212-2218.
18   C. Gong, Q. Wu, Y. Wang, D. Zhang, F. Luo, X. Zhao, Y. Wei and Z. Qian, *Biomaterials*, 2013, *34*, 6377-6387; X. Hu, H. Tan, P. Chen, X. Wang and J. Pang, *Journal of nanoscience and nanotechnology*, 2016, **16**, 5480-5488; C. Lu, R. B. Yoganathan, M. Kociolek and C. Allen, *Journal of pharmaceutical sciences*, 2013, **102**, 627-637.
19   A. C. Farthing and R. J. Reynolds, *Nature*, 1950, **165**, 647.
20   G. Vandermeulen, L. Rouxhet, A. Arien, M. E. Brewster and V. Preat, *International journal of pharmaceutics*, 2006, **309**, 234-240.
21   a) T. J. Deming, *Nature* **1997**, *390*, 386-389; b) T. J. Deming, *Adv. Drug Deliv. Rev.* **2002**, *54*, 1145-1155.
22   T. Yang, W. Li, X. Duan, L. Zhu, L. Fan, Y. Qiao and H. Wu, *PloS one*, 2016, **11**, e0162607.
23   a) A. Acharya, B. Ramanujam, A. Mitra, C. P. Rao, *ACS nano* **2010**, *4*, 4061-4073; b) K. L. Copeland, J. A. Anderson, A. R. Farley, J. R. Cox, G. S. Tschumper, *J. Phys. Chem. B* **2008**, *112*, 14291-14295; c) K. Jitsukawa, A. Katoh, K. Funato, N. Ohata, Y. Funahashi, T. Ozawa, H. Masuda, *Inorg. Chem.* **2003**, *42*, 6163-6165; d) M. Yoshikawa, H. Iwasaki, H. Shinagawa, *J. Biol. Chem.* **2001**, *276*, 10432-10436.
24   A. M. Puertas, F. J. de las Nieves, *J. Colloid Interface Sci.* **1999**, *216*, 221-229.
25   D. T. Haynie, S. Balkundi, N. Palath, K. Chakravarthula, K. Dave, *Langmuir* **2004**, *20*, 4540-4547.
26   a) B. Cheppudira, M. Fowler, L. McGhee, A. Greer, A. Mares, L. Petz, D. Devore, D. R. Loyd, J. L. Clifford, *Expert Opin. Investig. Drugs* **2013**, *22*, 1295-1303; b) K. K. Chereddy, R. Coco, P. B. Memvanga, B. Ucakar, A. des Rieux, G. Vandermeulen, V. Preat, *J. Control. Release* **2013**, *171*, 208-215; c) M. Panchatcharam, S. Miriyala, V. S. Gayathri, L. Suguna, *Mol. Cell. Biochem.* **2006**, *290*, 87-96.
27   a) K. S. Akers, M. P. Rowan, K. L. Niece, J. C. Graybill, K. Mende, K. K. Chung, C. K. Murray, *BMC Infect. Dis.* **2015**, *15*, 184; b) D. A. Sanchez, D. Schairer, C. Tuckman-Vernon, J. Chouake, A. Kutner, J. Makdisi, J. M. Friedman, J. D. Nosanchuk, A. J. Friedman, *Nanomedicine* **2014**, *10*, 269-277; c) O. Tabbene, S. Azaiez, A. Di Grazia, I. Karkouch, I. Ben Slimene, S. Elkahoui, M. N. Alfeddy, B. Casciaro, V. Luca, F. Limam, M. L. Mangoni, *J. Appl. Microbiol.* **2016**, *120*, 289-300.
28   a) F. Gaudiere, S. Morin-Grognet, L. Bidault, P. Lembre, E. Pauthe, J. P. Vannier, H. Atmani, G. Ladam, B. Labat, *Biomacromolecules* **2014**, *15*, 1602-1611; b) B. Manickam, R. Sreedharan, M. Elumalai, *Curr Drug Deliv.* **2014**, *11*, 139-145; c) A. P. Mathew, K. Oksman, D. Pierron, M. F. Harmand, *Macromol. Biosci.* **2013**, *13*, 289-298;
29   a) R. Baumeister, G. Muller, B. Hecht, W. Hillen, *Proteins* **1992**, *14*, 168-177; b) J. M. Richardson, M. M. Lopez, G. I. Makhatadze, *Proc. Natl. Acad. Sci. U.S.A* **2005**, *102*, 1413-1418.
30   a) J. S. Chiou, T. Tatara, S. Sawamura, Y. Kaminoh, H. Kamaya, A. Shibata, I. Ueda, *Biochim. Biophys. Acta* **1992**, *1119*, 211-217; b) K. Fukushima, T. Sakamoto, J. Tsuji, K. Kondo, R. Shimozawa, *Biochim. Biophys. Acta* **1994**, *1191*, 133-140; c) J. Rao, Z. Luo, Z. Ge, H. Liu, S. Liu, *Biomacromolecules* **2007**, *8*, 3871-3878; d) J. Sun, C. Deng, X. Chen, H. Yu, H. Tian, J. Sun, X. Jing, *Biomacromolecules* **2007**, *8*, 1013-1017.
31   V. T. Huynh, G. Chen, P. d. Souza, M. H. Stenzel, *Biomacromolecules* **2011**, *12*, 1738-1751.
32   C. F. van Nostrum, *Soft Matter* **2011**, *7*, 3246-3259.
33   a) M. Koskela, F. Gaddnas, T. I. Ala-Kokko, J. J. Laurila, J. Saarnio, A. Oikarinen, V. Koivukangas, *Crit. Care* **2009**, *13*, R100; b) R. M. Rico, R. Ripamonti, A. L. Burns, R. L. Gamelli, L. A. DiPietro, *J. Surg. Res.* **2002**, *102*, 193-197.
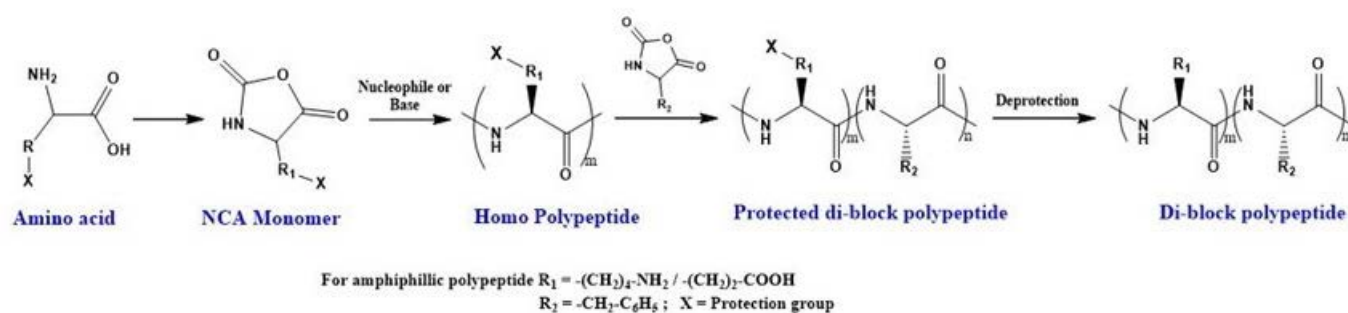
Journal Name

ARTICLE
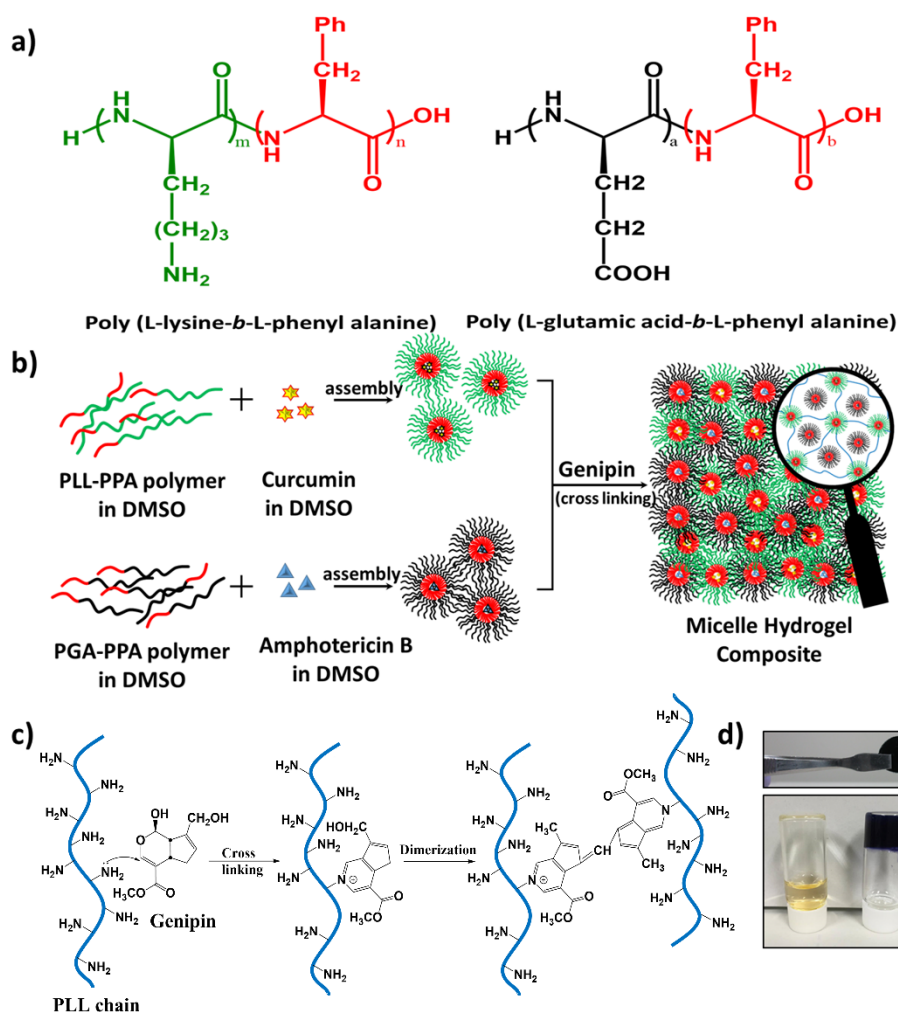
Figure 1. Preparation of micelle hydrogel composite. (a) Schematic structure of prepared copolymers. (b) Schematic representation of composite preparation based on genipin crosslinking. (c) Schematic representation of crosslinking by genipin and (d) photograph of the genipin crosslinked micelle-hydrogel composite before and after gelation and as a self-standing gel.

Table 1. Overview of polypeptides synthesized using NCA amino acid polymerization.

Polymer	DP		M_n X 10^3	PDI[b]	CMC (mg mL^{-1})	Micelle size[c] (nm)
	Block a (PLL / PGA)	Block b (PPA)				
PLL$_{200}$-PPA$_5$	187	4.1	51.13	1.17	0.67	472
*PLL$_{100}$-PPA$_5$	91	4.7	28.93	1.23	0.22	196
PGA$_{200}$-PPA$_5$	193	3.9	35.80	1.32	0.43	368
*PGA$_{100}$-PPA$_5$	88	4.3	18.33	1.15	0.15	173

For amphiphillic polypeptide R_1 = -(CH$_2$)$_4$-NH$_2$ / -(CH$_2$)$_2$-COOH
R_2 = -CH$_2$-C$_6$H$_5$; X = Protection group

Scheme 1: Representation of the preparation of polypeptides by ring opening polymerization of NCA and subsequent de-protection.
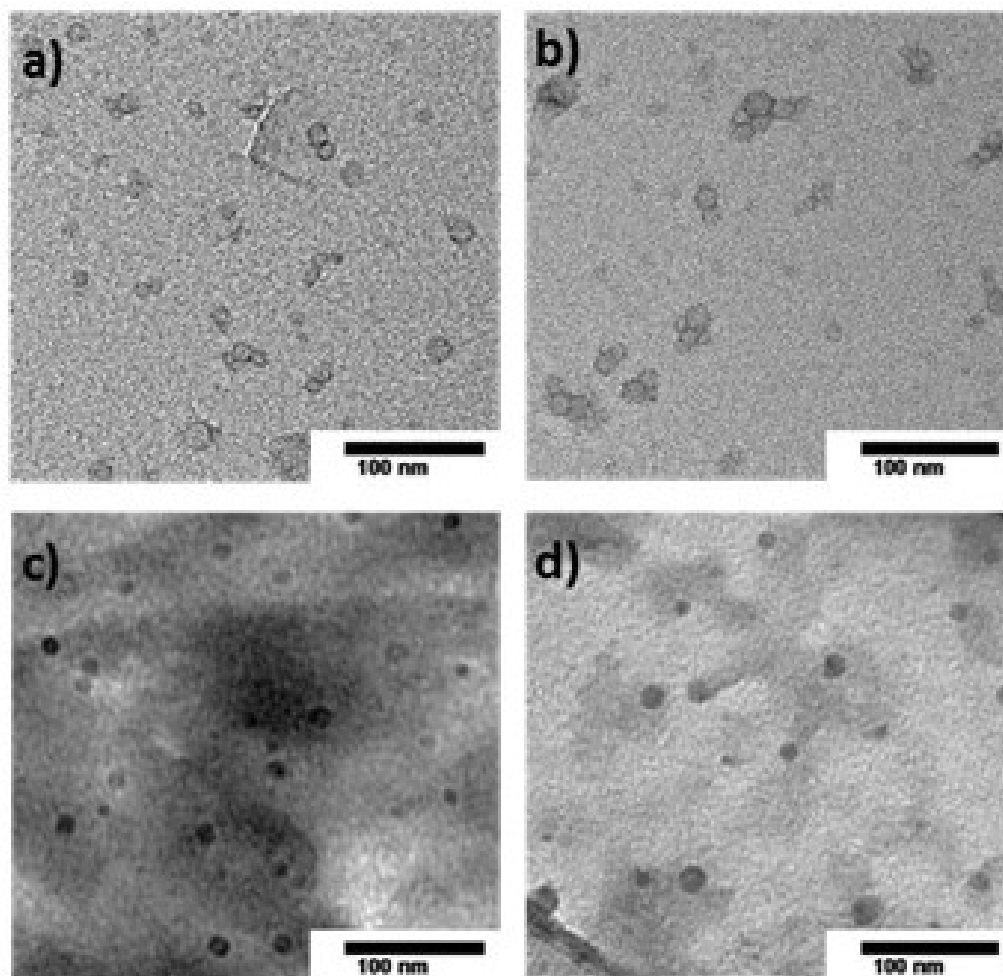
Figure 2. Particle size characterization of prepared micelles by transmission electron microscopy. (a) and (c) show PGA-PPA micelles before and after Amphotericin B loading and (b) and (d) show PLL-PPA micelles before and after loading of curcumin.
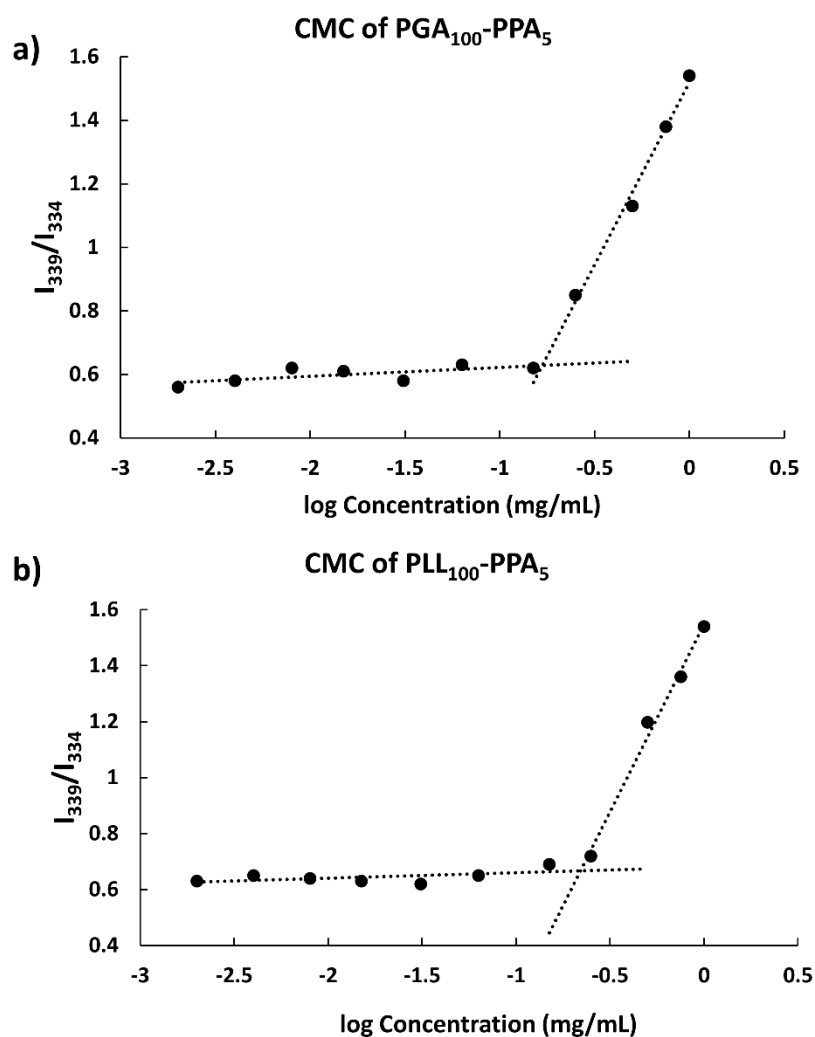
Figure 3: CMC determination of (a) PGA-PPA and (b) PLL-PPA. Intensity ratio (339/334) of pyrene vs. logarithm concentration of polypeptide.
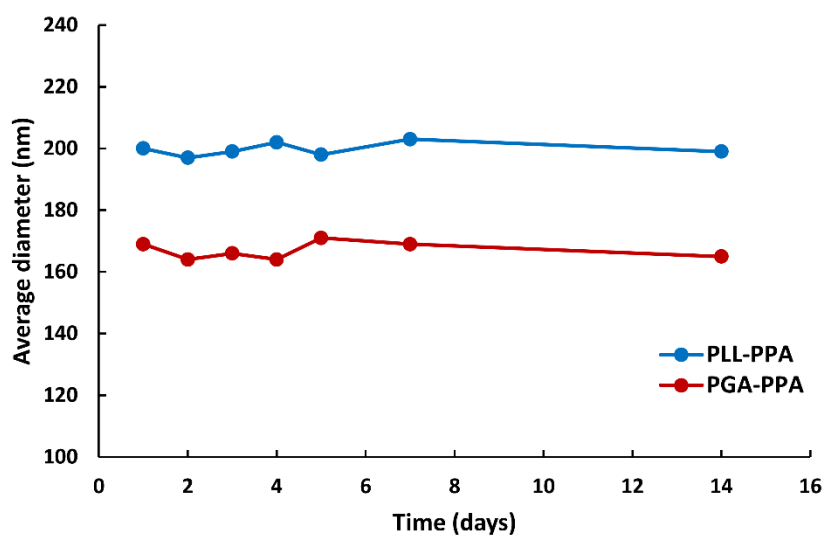
Figure 4: Stability of micelles over time. Diameter as observed by DLS shows fair stability of micelles with almost no aggregation.
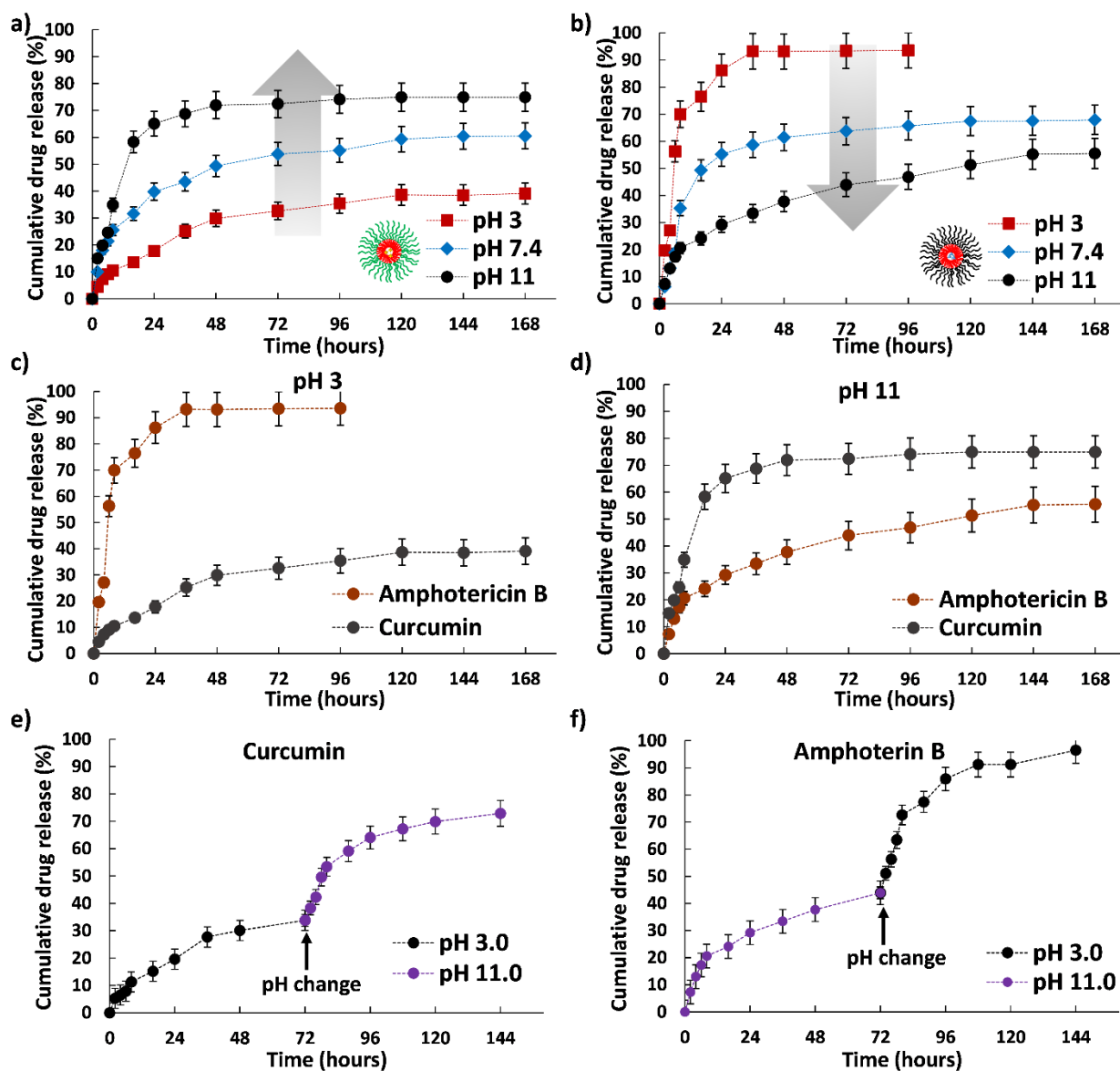
Figure 5: In vitro drug release profiles of the polymer micelles at different pH and crosslinking values (pH 3.0, 7.4, and 11) at constant cross linker concentration (1% of genipin). (a) Curcumin; (b) amphotericin B; and (c) and (d) switchability of drug release profiles at pH 3 and 11, respectively. (e) and (f) show the biphasic release of drugs from composites, when the surrounding buffer was switched from one pH to another.
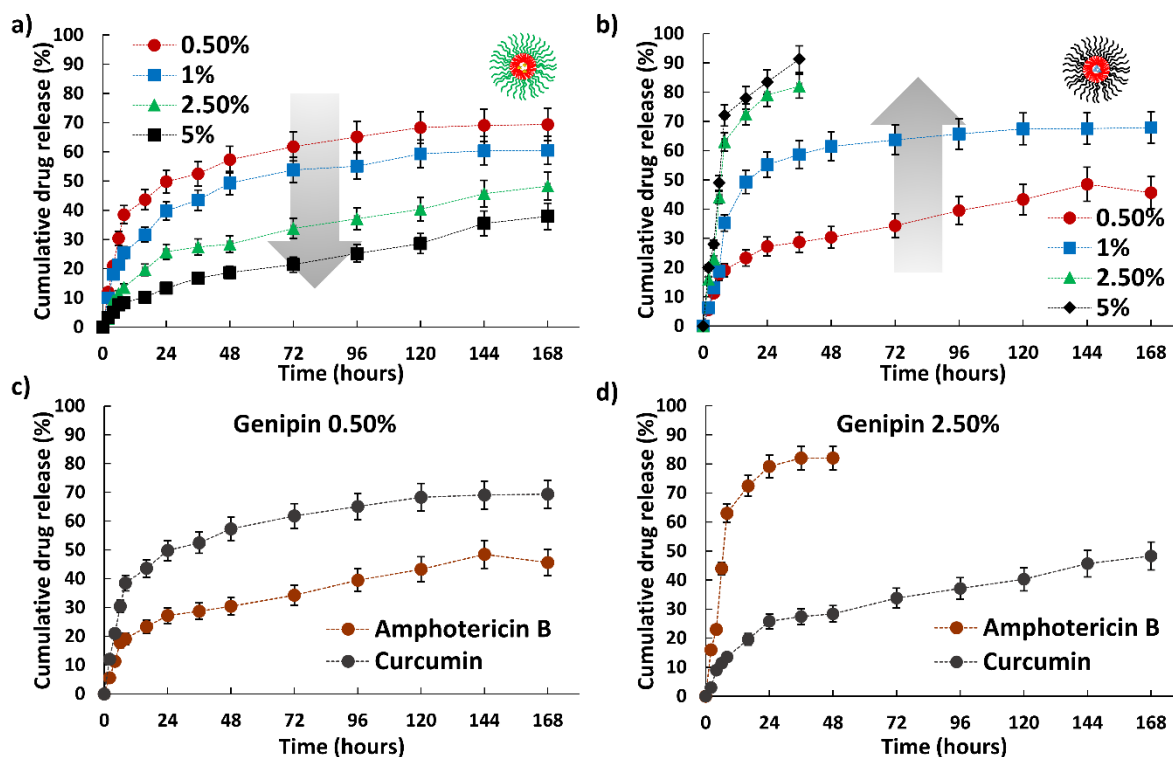
Figure 6: *In vitro* drug release profiles of the polymer micelles at different crosslinking values at pH 7.4. (a) Curcumin; (b) amphotericin B; and (c) and (d) release profile switching at different cross linker concentrations.
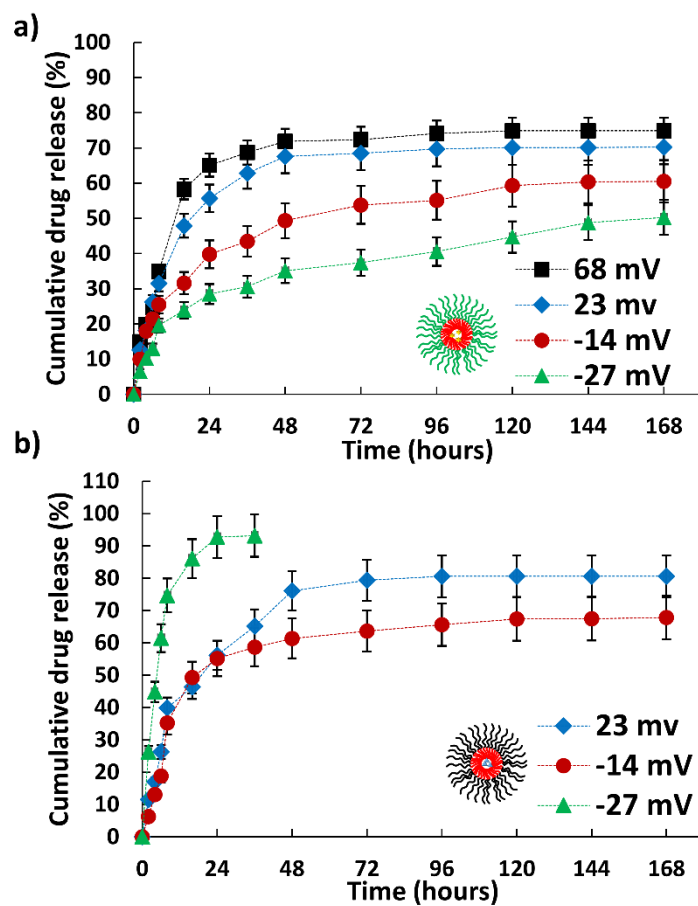
Figure 7: Percent drug release against time from (a) curcumin release from loaded PLL-PPA micelles and (b) amphotericin B release from loaded PGA-PPA micelles, at different ζ-potentials.

Switchable release nano-reservoirs for co-delivery of drugs via a facile micelle-hydrogel composite

Monika Patel[a], Tatsuo Kaneko[b] and Kazuaki Matsumura[a]*

[a] Materials Chemistry Area, School of Materials Science,
Japan Advanced Institute of Science and Technology, 1-1 Asahidai, Nomi, Ishikawa
923-1292, Japan
[b] Energy and Environment Area, School of Materials Science,
Japan Advanced Institute of Science and Technology, 1-1 Asahidai, Nomi, Ishikawa
923-1292, Japan

E-mail: mkazuaki@jaist.ac.jp
Ph. : +81-761-51-1680

Figures
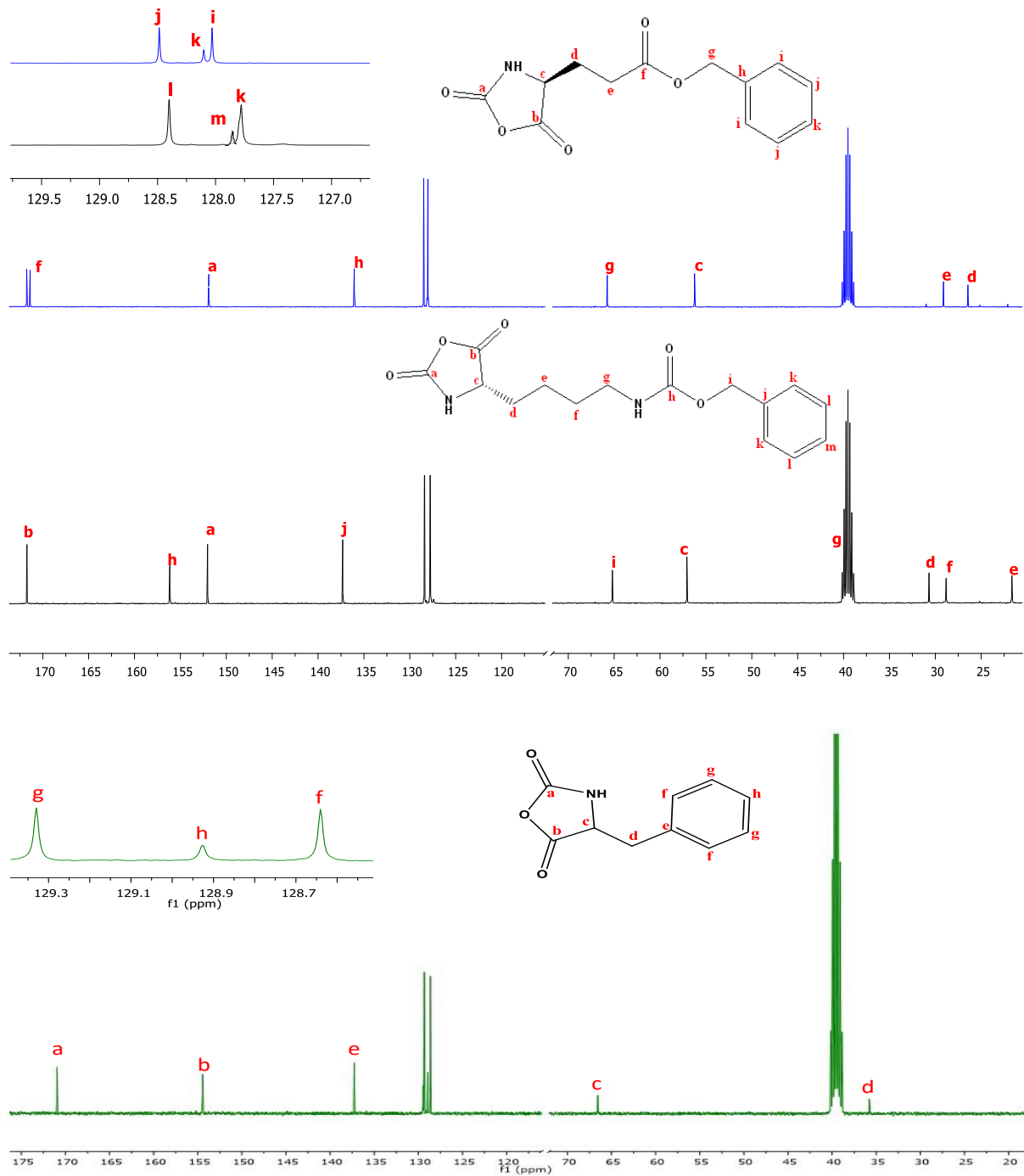
**Figure S1:** ^{13}C NMR of Glu (OBzl)-NCA [blue]; Lys(Z)-NCA [black] and Phe-NCA [green].
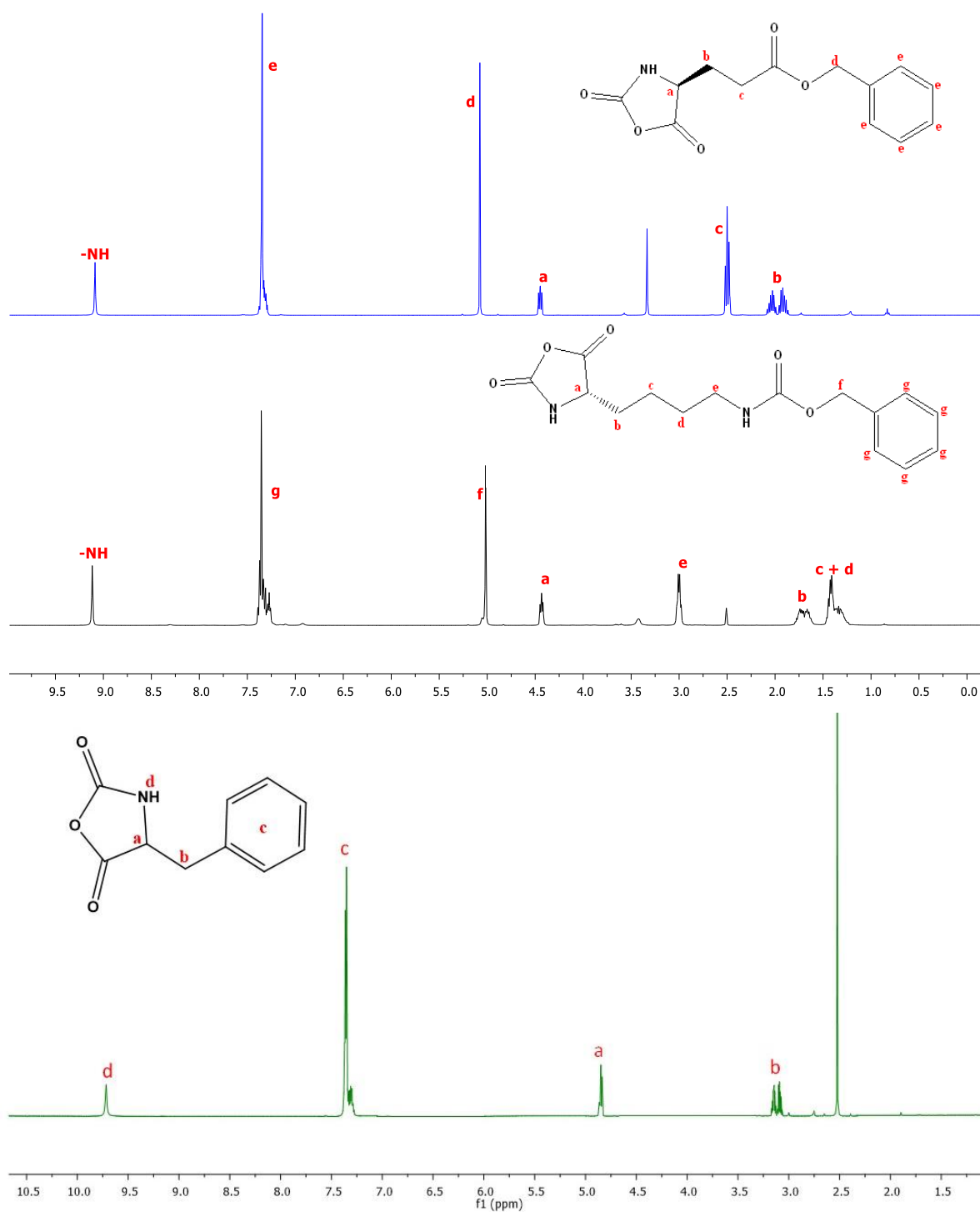
Figure S2: ^{1}H NMR of Glu (OBzl)-NCA [blue]; Lys(Z)-NCA [black] and Phe-NCA [green].
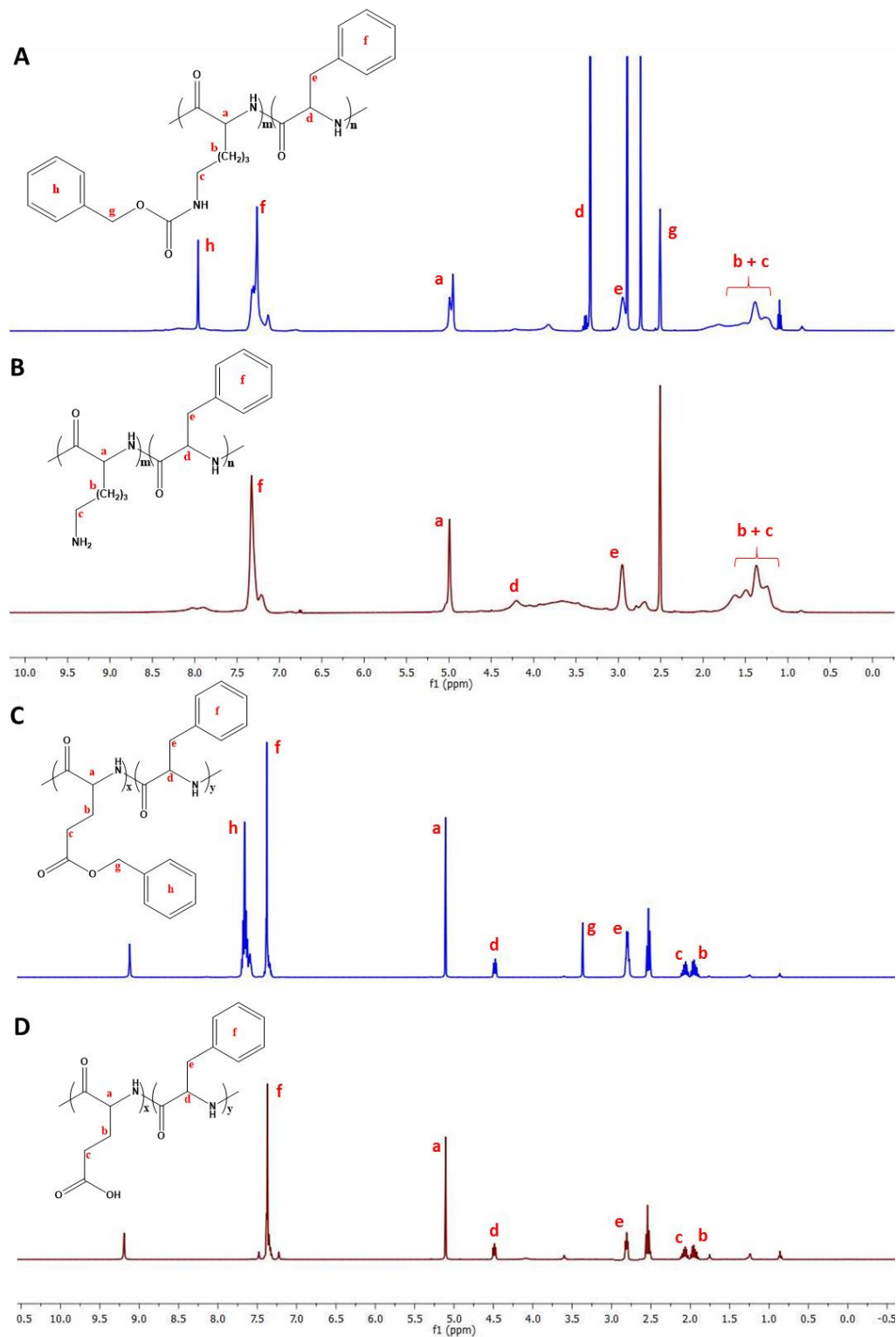
**Figure S3:** ^{1}H NMR of synthesized polymers A. PLL-PPA (poly L lysine-b-poly phenylalanine) protected; B. PLL-PPA deprotected; C. PGA-PPA (poly glutamic acid-b-poly phenylalanine) protected and D. PGA-PPA deprotected.
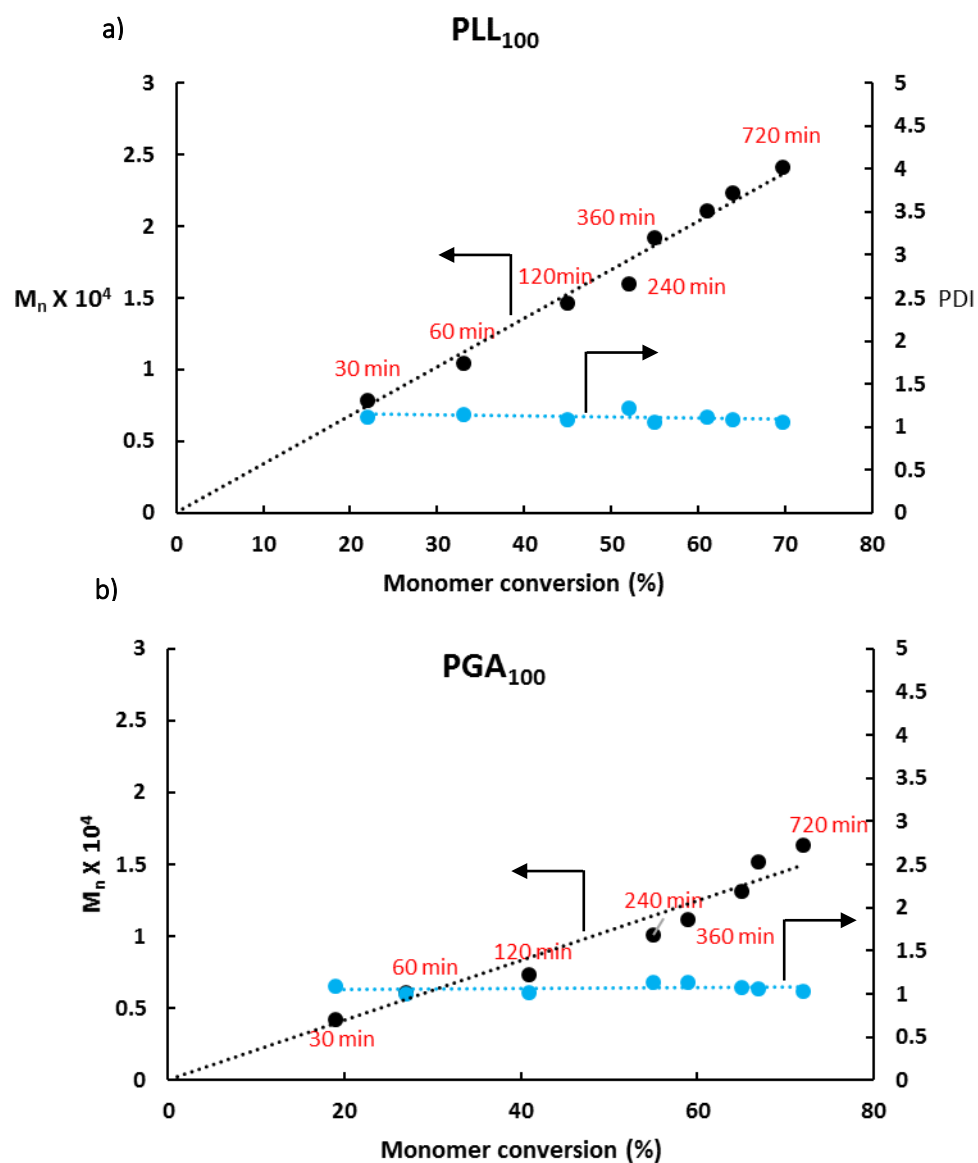
Figure S4: Molecular weight (M_n) and the PDI as a function of monomer conversion showing the controllability of the polymerization reaction; **a.** PLL block and **b.** PGA block
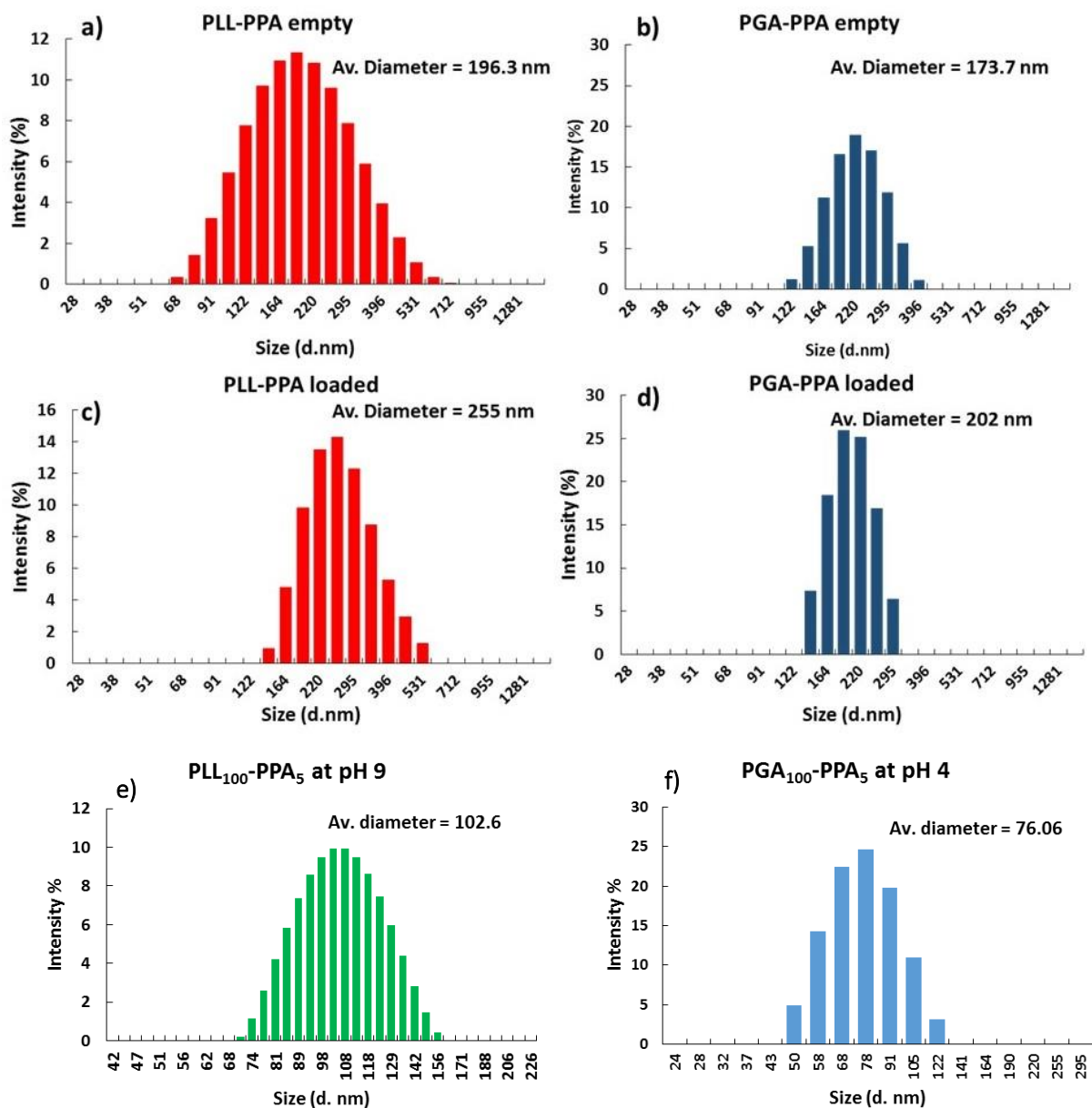
Figure S5: Dynamic Light Scattering (DLS) results (a) and (c) show PLL-PPA micelles before and after curcumin loading; (b) and (d) show PGA-PPA micelles before and after loading of amphotericin B; (e) and (f) showing the change in hydrodynamic diameter of PLL_{100}-PPA_5 and PGA_{100}-PPA_5 at pH 9.0 and 4.0 respectively.
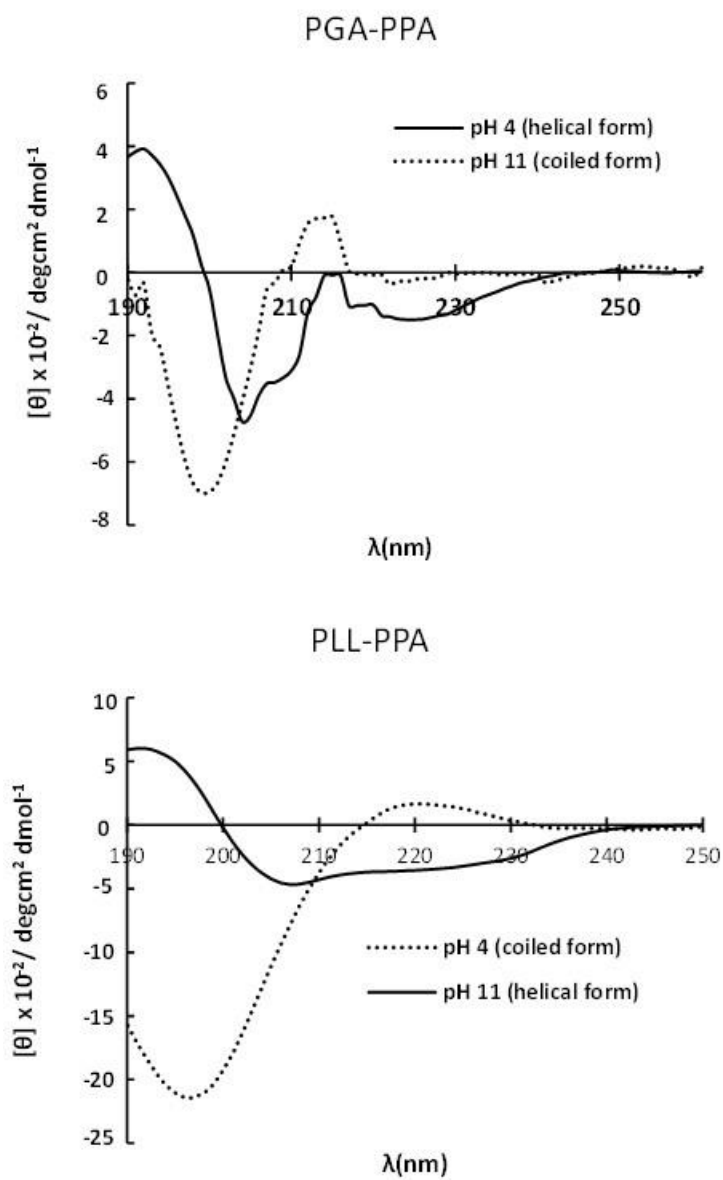
Figure S6: CD spectra of PGA-PPA (top) and PLL-PPA (bottom) at pH showing their respective transitions from random coil to α-helix at change in pH.
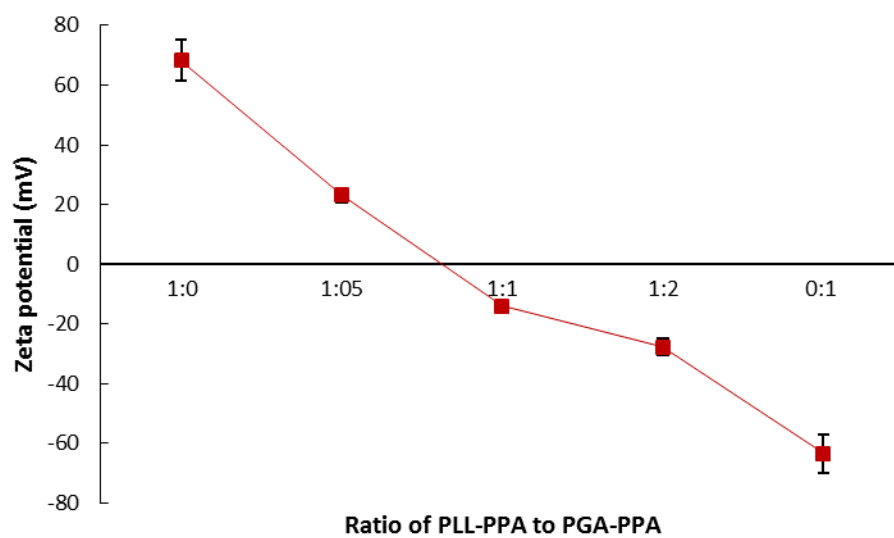
Figure S7: Variations in zeta potential of various ratios of PLL-PPA: PGA-PPA micelles.
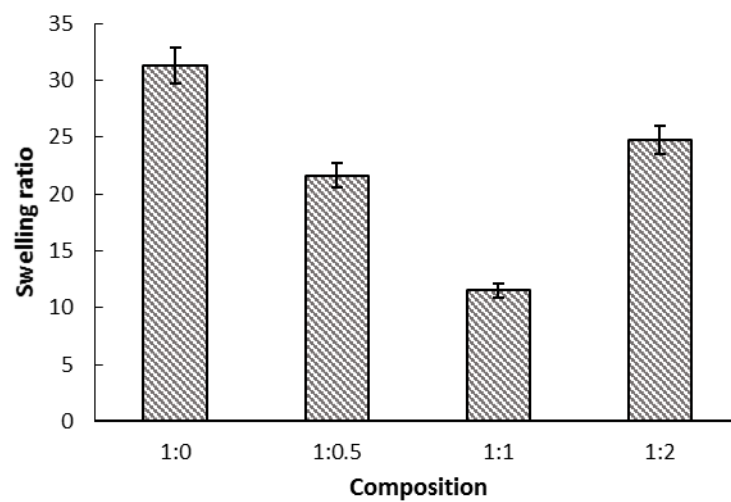
Figure S8: The equilibrium swelling ratios of the composites with varying ratios of PLL-PPA: PGA-PPA. (n=3)